MicroRNA-223-induced inhibition of the *FBXW7* gene affects the proliferation and apoptosis of colorectal cancer cells via the Notch and Akt/mTOR pathways

ZHIXIN LIU[1-3], TENG MA[1], JUFENG DUAN[1], XIAOFEI LIU[1] and LONG LIU[1,3]

Departments of [1]Infectious Diseases and [2]Respiratory Medicine, [3]School of Basic Medical Sciences, Renmin Hospital, Hubei University of Medicine, Shiyan, Hubei 442000, P.R. China

Received May 5, 2020; Accepted November 17, 2020

DOI: 10.3892/mmr.2020.11793

Abstract. The tumour suppressor gene F-box and WD repeat domain-containing 7 (*FBXW7*) plays an important role in human cancer by regulating cell division, proliferation and differentiation. However, the exact regulatory mechanisms of microRNA (miR)-223 in colorectal cancer (CRC) cells are still unknown. The present study aimed to investigate the effect and mechanism of miR-223 inhibiting *FBXW7* on the proliferation and apoptosis of CRC cells. HCT116 cells were transfected with miR-223 mimics or small interfering RNA (siRNA) targeting *FBXW7* (si*FBXW7*), and the effects of these treatments on cell proliferation and apoptosis were examined. The downstream Notch and Akt/mTOR pathways were also assessed. Following miR-223 overexpression, the mRNA and protein expression levels of FBXW7 were downregulated. Transfection with miR-223 mimics or si*FBXW7* promoted the proliferation of HCT116 cells and inhibited apoptosis by promoting the Notch and Akt/mTOR signalling pathways. Conversely, miR-223 mimics transfection with FBXW7 overexpression inhibited cell viability and restored apoptosis. Thus, the present study demonstrated that miR-223 could bind to the *FBXW7* gene and inhibit its expression, ultimately increasing the proliferation and preventing the apoptosis of CRC cells through the Notch and Akt/mTOR signalling pathways.

Introduction

Colorectal cancer (CRC) is the third most common malignant tumour in China, and its mortality ranks fourth among all malignant tumours (1,2). At present, the first choice of treatment for CRC is surgical resection. However, the optimal time window for surgery is often missed when the early symptoms of CRC are not detected; thus, early screening for the diagnosis of CRC is key to improving treatment outcomes (3). Identifying a marker that is specific to CRC and easy to detect would provide new insight for the early diagnosis, treatment and monitoring of CRC.

F-box and WD repeat domain-containing 7 (FBXW7) is a novel ubiquitin ligase encoded by the tumour suppressor gene *FBXW7*. Its active targets consist of a variety of cancer-related factors, such as cyclin E, c-Myc, Mcl-1, c-Jun and mTOR (4,5). Abnormal expression of these targets is associated with CRC, gastric cancer and ovarian cancer (6). FBXW7 plays a role in physiological and pathological processes, such as tumour cell proliferation, early apoptosis and signal transduction (7,8). Previous studies have indicated that the expression of *FBXW7* serves an indispensable role in the occurrence, development and metastasis of CRC (9-11).

MicroRNAs (miRNAs/miRs) are involved in a wide range of cellular functions and normal biological processes, including cell proliferation, differentiation, apoptosis and biotic stress resistance (12,13). Notably, some miRNAs are considered to have oncogenic activities, while others act as tumour suppressors (14,15). Oncogenic miRNAs are upregulated in cancer and promote cancer development by targeting tumour suppressor genes through different mechanisms. For instance, previous studies have identified a negative correlation between miR-223 expression and FBXW7 expression in breast cancer, hepatocellular carcinoma, non-small cell lung cancer and CRC (16-19). Monitoring miRNAs that bind to the *FBXW7* gene, and regulate CRC development and progression, could be an important approach for the prognosis of clinical treatment effects. However, the precise regulatory mechanisms underlying the effects of miR-223 on CRC progression remain unclear.

Notch signalling is an evolutionarily conserved pathway that is involved in various processes, including cell proliferation, differentiation and apoptosis (20). Notch signalling is also considered to be associated with tumorigenesis (21). Increasing evidence has revealed that Notch1 is relevant to other signalling pathways, such as Akt/mTOR and NF-κB signalling (22,23). In addition, miRNAs have been reported

Correspondence to: Dr Long Liu, School of Basic Medical Sciences, Renmin Hospital, Hubei University of Medicine, 30 South Renmin Road, Shiyan, Hubei 442000, P.R. China
E-mail: liulong2015@outlook.com

Key words: colorectal cancer, F-box and WD repeat domain containing 7, microRNA-223, Notch pathway, Akt/mTOR pathway, proliferation, apoptosis

to regulate genes within the Notch and mTOR signalling pathways (24,25); therefore, the miR-223/FBXW7 axis may be associated with Notch/mTOR signaling.

The aim of the present study was to examine the regulatory relationship between miRNAs, FBXW7 and associated signalling pathways in order to improve current understanding of the mechanisms underlying CRC progression. The present study demonstrated that miR-223 was upregulated in CRC tissue and could bind to the 3'untranslated region (UTR) of the *FBXW7* gene. miR-223 also promoted HCT116 cell proliferation, whilst inhibiting apoptosis.

Materials and methods

Clinical samples. A total of 20CRC primary tumour tissue samples and matched adjacent non-tumour tissues were collected at the Affiliated Renmin Hospital of Hubei University of Medicine (Shiyan, China) between October 2016 and December 2018. All patients were diagnosed in histopathologically and clinically according to the American Joint Committee on Cancer criteria, and performed surgical operation. The adjacent tissue was 5 cm away from the edge of the tumour, all the tissue samples were snap frozen using liquid nitrogen, and then stored at -80˚C until further analysis. This research was approved by the Ethics Committee of Hubei University of Medicine, and all patients provided written informed consent for the use of samples.

Plasmid construction. The *FBXW7* gene was cloned into pTriEx-1.1 vector. The 3'UTR of the *FBXW7* gene was inserted into pMIR-REPORT vector (Ambion) to construct the recombinant plasmids for luciferase reporter gene assays. The primers used for PCR are listed in Table SI. The pTriEx-1.1 (Novagen) and pMIR-REPORT vectors were separately digested with *Hin*dIII/*Sac*I or *Nco*I/*Bam*HI, respectively, then the digested fragments were ligated with T4 DNA Ligase (New England Biolabs, Inc.) after purification. The recombinant plasmids were transformed into *Escherichia coli* and screened by PCR, and their sequences verified by sequencing.

Bioinformatics analysis. The potential miRNAs targeting the *FBXW7* gene (including its UTR) were analysed by TargetScan (version 7.1; www.targetscan.org/). Target miRNA expression was predicted using miRanda (www. microrna.org/microrna/). The bioinformatics analyses, including expression and prognosis, were performed by Sangerbox (http://sangerbox.com/Tool) using the pan-cancer monogenic fast comprehensive analysis tool. The expression data of normal mucosa tissues and CRC tissues were obtained from Genotype-Tissue Expression (GTEx, https://gtexportal.org/home/) and The Cancer Genome Atlas (TCGA, https://www.cancer.gov/about-nci/organization/ccg/research/structural-genomics/tcga). Differential gene expression levels was calculated as the $\log_2$ of its upper quartile Fragments Per Kilobase of transcript per Million mapped reads value. The expression levels of *FBXW7* mRNA were calculated as the $\log_2$ of its TPM (transcripts per million) value after normalization of gene length and sequencing depth.

Immunohistochemistry staining. The procedures for immunohistochemistry staining were performed as previously reported (26). Sections (3-μm thick) were fixed using 4% paraformaldehyde for 12 h. The paraformaldehyde-fixed, paraffin-embedded sections were deparaffinized and rehydrated, and antigen retrieval was performed in boiling citrate buffer for 10 min, followed by blocking with 3% hydrogen peroxide for 10 min at room temperature. After washing with PBS three times, the sections were incubated with anti-FBXW7 antibody (1:200; Abcam; cat. no. ab109617) overnight at 4˚C. The secondary antibody (1:50; Beyotime Institute of Biotechnology; cat. no. A0208) was incubated for 1 h at room temperature, followed by incubation with 3-diaminobenzidine (DAB) and re-staining with haematoxylin. The staining results were photographed under a BX46 light microscope (Olympus Corporation) and evaluated by two pathologists in a blinded manner.

Cell culture and transfection. The human HCT116 cell line was purchased from American Type Culture Collection and cultured in high-glucose DMEM (Thermo Fisher Scientific, Inc.) containing 10% FBS (Gibco; Thermo Fisher Scientific, Inc.) in a 37˚C incubator with 5% CO_2. Cells in the logarithmic growth phase (80% confluence) were used for experiments. The 50 ng pMIR-REPORT luciferase reporter plasmids (Ambion; 50 ng), miR-223 mimics (5'-UGUCAGUUUGUCAAAUACCCCA-3'), miR mimic control (miCtr, 5'-UUCUCCGAACGUGUCACGUTT-3'), miR-223 inhibitor (5'-UGGGGUAUUUGACAAACUGACA-3') and miR-223 inhibitor control (Ctr; 5'-CAGUACUUUUGUGUAGUACAA-3') were transfected using Lipofectamine® 2000 (Invitrogen; Thermo Fisher Scientific, Inc.). Small interfering RNA (siRNA) targeting *FBXW7* (si*FBXW7*-1, 5'-ACAGGACAGUGUUUACAAA-3'; si*FBXW7*-2, 5'-CCAUGCAAAGUCUCAGAAU-3') and negative control (si-NC, 5'-UUCUCCGAACGUGUCACGUTT-3') were transfected using Entranster™-R4000 (Engreen Biosystem, Ltd.), according to the manufacturer's instructions. All small nucleic acids were purchased from Shanghai GenePharma Co., Ltd. and were used at a final concentration of 20 nM. The cells were treated or collected at the indicated times after transfection.

Luciferase reporter gene assay. The 3'UTR sequences of *FBXW7* were cloned into the pMIR-REPORT vector to construct the *FBXW7* luciferase reporter plasmids. A total of 50 ng reporter plasmids were co-transfected with 20 nM miR-223 mimics, miR-25 mimics, miR-223 inhibitor and mimics control (miCtr) into 293T cells. Luciferase activity was measured 36 h later by fluorescence detection with the Luciferase Assay System (Promega Corporation). The cells in the plate were lysed with 5Xcell lysis reagent (Promega Corporation). After centrifugation, the supernatant was collected and added to 100 μl luciferase assay reagent at room temperature, and luciferase was measured using a Glomax 20/20 bioluminescence detector (Promega Corporation). The luciferase activity was normalized to the activity of *Renilla* luciferase.

Cellular viability assay. The viability of HCT116 cells was detected using a Cell Counting Kit-8 (CCK-8) kit (Dojindo Molecular Technologies, Inc.). CCK-8 reagent (10 μl/well) was added to $1x10^6$ HCT116 cells/well at 0, 24, 48 and 72 h

post-transfection, which were then incubated at 37˚C with 5% CO_2 for 2 h. The absorbance was measured in each well at a wavelength of 450 nm using the xMark Microplate Absorbance Spectrophotometer (Bio-Rad Laboratories, Inc.). Each group was set up in triplicate.

Apoptosis assay. HCT116 cells transfected with miR-223 mimics or inhibitor were analysed using an Annexin V-fluorescein isothiocyanate (FITC)/propidium iodide (PI) Apoptosis Staining Kit (cat. no. ab14085; Abcam). A total of $1x10^6$ HCT116 cells from each group were collected 48 h post-transfection. After washing twice with PBS, the cells were resuspended in 500 μl binding buffer, then mixed with 5 μl Annexin V-FITC followed by 5 μl PI and incubated in the dark for 10 min at room temperature. Apoptosis in each group was detected by flow cytometry (Beckman Coulter, Inc.; CytoFLEX), the frequency of apoptotic cells (Annexin V^+PI^+) was obtained using software CytExpert 2.4 (Beckman Coulter, Inc.). The experiment was independently repeated three times.

FBXW7 rescue assay. A total of $1x10^6$ HCT116 cells/well were transfected with miR-223 mimics or NC using Entranster™-R4000 (Engreen Biosystem, Ltd.), then transfected with 1 μg pTriEx-*FBXW7* overexpression plasmid or empty plasmid 12 h later. The cells were collected 48 h later and lysed for protein detection by western blotting. The cell viability was also detected at the indicated times following miR-223 transfection and apoptosis rates were detected by flow cytometry at 48 h post-transfection.

RNA extraction and reverse transcription-quantitative (RT-q) PCR. Total RNA was extracted from homogenised tissue samples or from HCT116 cells harvested 36 h after transfection using TRIzol® (Invitrogen; Thermo Fisher Scientific, Inc.). cDNA was obtained using a OneScript cDNA Synthesis kit (Applied Biological Materials Inc., cat. no. G594) with an oligo(dT) primer or miRNA-specific stem-loop primers, according to manufacturer's protocol. The primers for RT and qPCR are listed in Table SI. mRNA expression levels were examined on an CFX96 Touch PCR system (Bio-Rad Laboratories, Inc.) using SYBR Premix Ex Taq™ (Applied Biological Materials Inc., G892). The thermocycling conditions were as follows: 95˚C for 30 sec, followed by 40 cycles at 95˚C for 5 sec and 60˚C for 30 sec. *GAPDH* or *U6* were used as the internal reference for genes or miRNAs, respectively. Each reaction was set up in triplicate, and experiments were performed three times. The relative expression of each target was analysed using the $2^{-\Delta\Delta Cq}$ method (27).

Western blot analysis. Total proteins of each group were collected from HCT116 cells 48 h post-transfection or from homogenised tissue and lysed using RIPA reagent (Solarbio), then quantified using a BCA kit (Beyotime Institute of Biotechnology). Proteins were separated by SDS-PAGE on 10% gels and transferred to PVDF membranes (Bio-Rad Laboratories, Inc.). The membranes were then blocked at 37˚C for 1 h using 5% skimmed milk and incubated at 4˚C overnight with mouse or rabbit anti-human polyclonal antibodies specific for FBXW7 (1:2,000; ProteinTech Group, Inc.; cat. no. 28424-1-AP), Notch intracellular receptor domain (NICD; 1:500; GeneTex, cat. no. GTX28925), hes family bHLH transcription factor 1 (Hes-1; 1:1,000; GeneTex; cat. no. GTX108356) and phosphorylated (p)-mTOR (1:1,000; GeneTex; cat. no. GTX132803). Antibodies specific for Akt (cat. no. 10176-2-AP), p-Akt (cat. no. 66444-1-Ig), mTOR (cat. no. 66888-1-Ig, ProteinTech Group, Inc.) was used at 1:2,000 dilution, and the mouse anti-human GAPDH monoclonal antibody was used at a 1:5,000 dilution (Beyotime Institute of Biotechnology; cat. no. AF5009). After washing the membrane three times, goat anti-mouse (cat. no. A0216) or anti-rabbit IgG (cat. no. A0208) (both at 1:5,000 dilution; Beyotime Institute of Biotechnology) was added, and the mixture was incubated for 1 h at room temperature, and then subjected to imaging using an ECL solution (Beyotime Institute of Biotechnology). Densitometric analysis of the protein bands was carried out using Image Lab 3.0 (Bio-Rad Laboratories, Inc.). Protein expression levels are presented as the ratio of the densitometric value of target proteins relative to the GAPDH internal control.

Statistical analysis. The cell viability, apoptosis and RT-qPCR results were statistically analysed using GraphPad Prism 5.0 software (GraphPad Software, Inc.). The data are presented as the mean ± SD of three independent experimental repeats. Comparisons between multiple groups were analysed using one-way ANOVA followed by the Tukey's HSD post hoc test. Student's t-test was used to compare two groups. $P<0.05$ was considered to indicate a statistically significant difference.

Results

Downregulation of FBXW7 expression in CRC. First, the present study investigated the difference in *FBXW7* expression in datasets from TCGA and GTEx databases representing 27 types of tumour tissue and adjacent normal tissue samples (Fig. 1A). FBXW7 expression was significantly downregulated in most tumour types, compared with adjacent tissue. Moreover, the expression of FBXW7 was evaluated in CRC tissue samples and adjacent normal tissue (n=20). The mRNA expression levels of *FBXW7* in CRC tissue were significantly lower than in normal tissues (Fig. 1B). The protein expression of FBXW7 was also lower in CRC tissues compared with in adjacent tissues (Fig. 1C and D). Immunohistochemical staining also suggested reduced expression in the cells of CRC tissue compared with in adjacent colon tissue (Fig. 1E). Disease-specific survival (DSS) and overall survival (OS) time of patients with CRC did not correlate with *FBXW7* expression (Figs. S1 and S2).

Upregulated miR-223 targets FBXW7 in CRC cells. miRNA sequences complementary to the human *FBXW7* gene were predicted using the TargetScan and miRanda (28) tools, which suggested miR-223, miR-22 and miR-25 targeted the 3'UTR of *FBXW7* (Fig. 2A). To determine the expression levels of the predicted miRNAs in CRC cells, the levels of miRNAs in HCT116 cells were measured using RT-qPCR. The relative expression level of miR-223 was significantly increased in CRC tissue compared with in adjacent tissues (Fig. 2B).

miR-223 binds to FBXW7 and inhibits its expression in HCT116 cells. A *FBXW7* luciferase vector was co-transfected

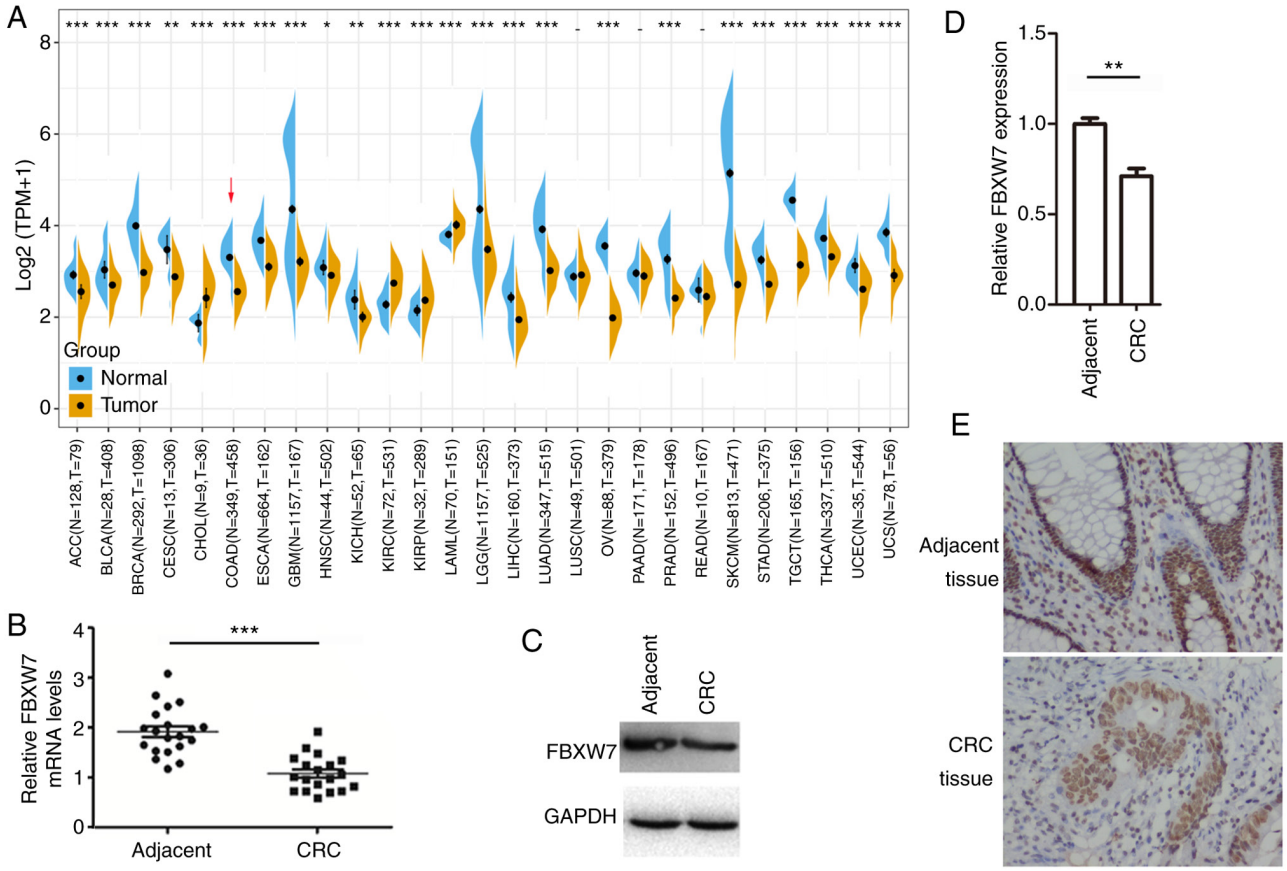

Figure 1. FBXW7 mRNA and protein expression levels in CRC tissues and adjacent normal tissues. (A) Differences in FBXW7 expression in 27 types of tumour tissue and normal tissue samples in The Cancer Genome Atlas and the Genotype Tissue Expression database. The red arrow marks the expression in CRC tissue, compared with healthy tissue. (B) *FBXW7* mRNA expression in CRC tissues and normal adjacent tissue. n=20 in each group. (C) FBXW7 protein expression in CRC tissue and normal adjacent tissue. (D) Western blotting results normalized to those of GAPDH levels. (E) Immunohistochemical staining of FBXW7 expression in CRC and normal adjacent tissues. Magnification, x200. Data are presented as the mean ± SD of three replicates. **P<0.01, ***P<0.001, vs. adjacent (paired Student's t-test). CRC, colorectal cancer; N, normal; T, tumour; FBXW7, F-box and WD repeat domain containing 7; $\log_2$(TPM+1), normalization of gene expression; TPM, transcripts per million.

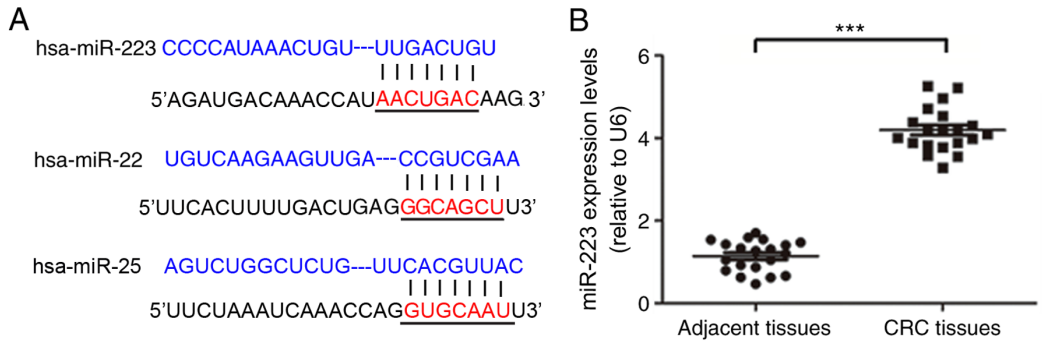

Figure 2. miR analysis and detection in CRC tissues and HCT116 cells. (A) miR molecules targeting the *FBXW7* gene were predicted using TargetScan and miRanda. miR sequences are marked in blue, and the *FBXW7* 3'UTR sequence was under them. The putative binding site is shown in red. (B) RT-qPCR detection of miR-223 levels in CRC tissues and adjacent normal tissues. n=20. ***P<0.001 (paired two-tailed Student's t-test). miR, microRNA; CRC, colorectal cancer; FBXW7, F-box and WD repeat domain containing 7; RT-qPCR, reverse transcription-quantitative PCR.

with miR-223 mimics, miR-25 mimics, miCtr or miR-223 inhibitor into 293T cells. Changes in luciferase activity in the transfected cells were measured 36 h post-transfection. miR-223 significantly reduced relative luciferase activity, while miR-25 did not influence luciferase activity (Fig. 3A). This indicates that miR-223 may interact with the 3'UTR of *FBXW7*. The effect of miR-223 on the expression of FBXW7 was evaluated in HCT116 cells. miR-223 mimics or inhibitor were used to transfect HCT116 cells (Fig. 3B). FBXW7 protein expression levels were decreased after transfection with miR-223 mimics compared with miCtr (Fig. 3C). mRNA expression levels were also significantly downregulated (Fig. 3C). However, FBXW7 protein and mRNA expression levels were not significantly altered after transfection with the

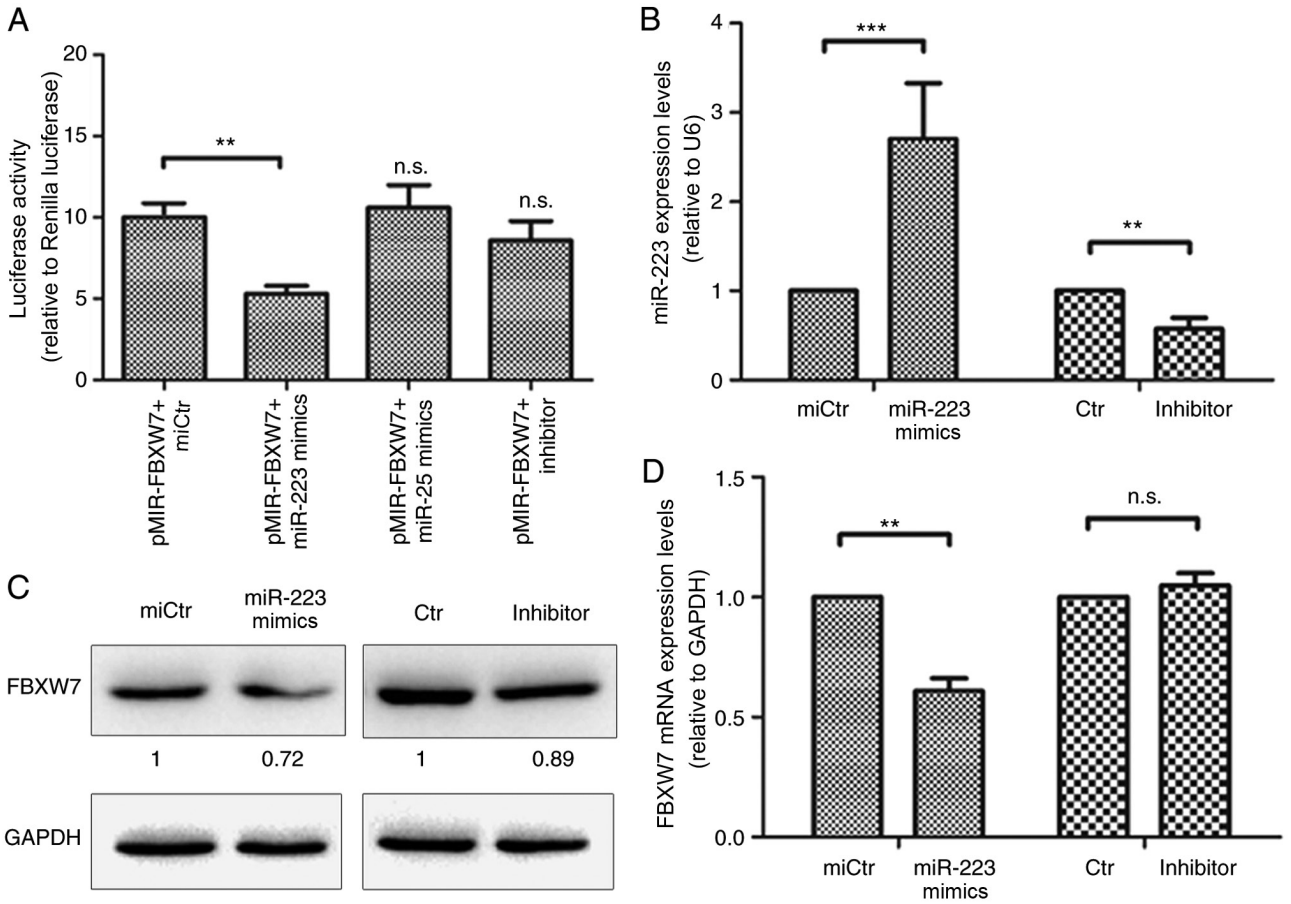

Figure 3. miR-223 inhibits the expression of FBXW7 in HCT116 cells. (A) miR-223 binding to *FBXW7* was detected using a luciferase reporter assay. Comparisons were made using Tukey's test. (B) miR-223 expression in HCT116 cells transfected with miR-223 mimics or inhibitor. (C) FBXW7 protein expression levels in HCT116 cells following transfection with miR-223 mimics or inhibitor. (D) *FBXW7* mRNA expression levels in HCT116 cells transfected with miR-223 or inhibitor. Data are presented as the mean ± SD of three replicates. **P<0.01, ***P<0.001 (one-way ANOVA). miR, microRNA; FBXW7, F-box and WD repeat domain containing 7. miCtr, mimics control; Ctr, inhibitor control; NC negative control; n.s., not significant.

inhibitor. This indicated that miR-223 could directly inhibit *FBXW7* expression.

Inhibition of FBXW7 by miR-223 affects the proliferation and apoptosis of HCT116 cells. To investigate the function of miR-223 targeting *FBXW7* in CRC cells, HCT116 cells were transfected with miR-223 mimics or inhibitor sequences, and cell viability was evaluated at different time points. Transfection with miR-223 mimics increased cell proliferation after transfection for 48 h, compared with miCtr (Fig. 4A). However, transfection with the inhibitor had no effect. In addition, apoptosis of HCT116 cells was detected by flow cytometry (Fig. 4B). Transfection with miR-223 mimics led to a decrease in the number of apoptotic cells, compared with miCtr, whereas the miR-223 inhibitor promoted apoptosis of HCT116 cells, compared with Ctr (Fig. 4C).

siRNA silencing of FBXW7 regulates HCT116 cell proliferation and apoptosis. siRNA targeting FBXW7 expression was used to further verify the effect of FBXW7 on HCT116 cell proliferation and apoptosis. Compared with si-NC, the relative mRNA and protein expression levels of FBXW7 were reduced after transfection with siFBXW7-1 and siFBXW7-2 (Fig. 5A and B). The cell viability assay indicated that siFBXW7-2 increased HCT116 cell proliferation, compared with si-NC (Fig. 5C). Moreover, compared with the control, both siRNA transfections reduced the apoptotic cell rate (Fig. 5E). In addition, rescuing FBXW7 through overexpression after transfection with miR-223 mimics inhibited cell viability and increased apoptosis compared with miR-223 mimics alone (Fig. 5D and G). FBXW7 protein levels were upregulated following co-transfection with *FBXW7* overexpression vector and miR-223 mimics, compared with mimics alone (Fig. 5F). Altogether, these results indicated that miR-223 may promote the proliferation and suppress the apoptosis of HCT116 cells by targeting FBXW7.

FBXW7 functions through the Notch and Akt/mTOR pathways. Multiple studies have demonstrated that FBXW7 plays a key role in cancer by regulating the Notch and mTOR pathways (29,30). Thus, the possible association between miR-223/*FBXW7* axis and Notch-mTOR signalling pathways was examined. Following transfection with miR-223 mimics or si*FBXW7*-2, the mRNA expression levels of *Notch* and its target gene *Hes-1* were increased, compared with miCtr + si-NC group (Fig. 6A and B), and the expression levels of NICD and Hes-1 were increased after inhibition of FBXW7 (Fig. 6C). The protein expression levels of total

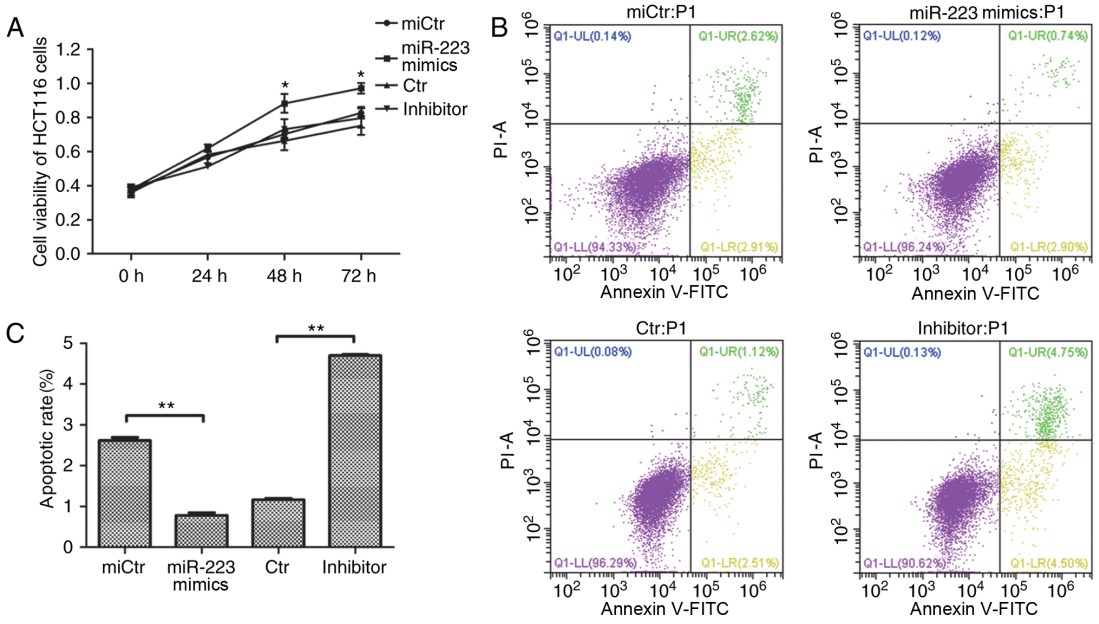

Figure 4. Effect of miR-223 on cell viability and apoptosis of HCT116 cells. (A) Effect of miR-223 mimics transfection on the activity of HCT116 cells. Cells were detected using the Cell Counting Kit-8 reagent after transfection with miR-223 mimics or inhibitor from 0 to 72 h. *P<0.05 vs. miCtr (one-way ANOVA and Tukey's post hoc test). (B) Effect of miR-223 mimics and inhibitor transfection on the early apoptosis of HCT116 cells. (C) Apoptosis rates were recorded following Annexin V-FITC/PI double staining. Data are presented as the mean ± SD of three replicates. **P<0.01 (one-way ANOVA and Tukey's post hoc test). miR, microRNA; FBXW7, F-box and WD repeat domain containing 7; miCtr, mimics control; Ctr, inhibitor control; FITC, fluorescein isothiocyanate; PI, propidium iodide; UL, upper left; UR, upper right; LL, lower left; LR, lower right.

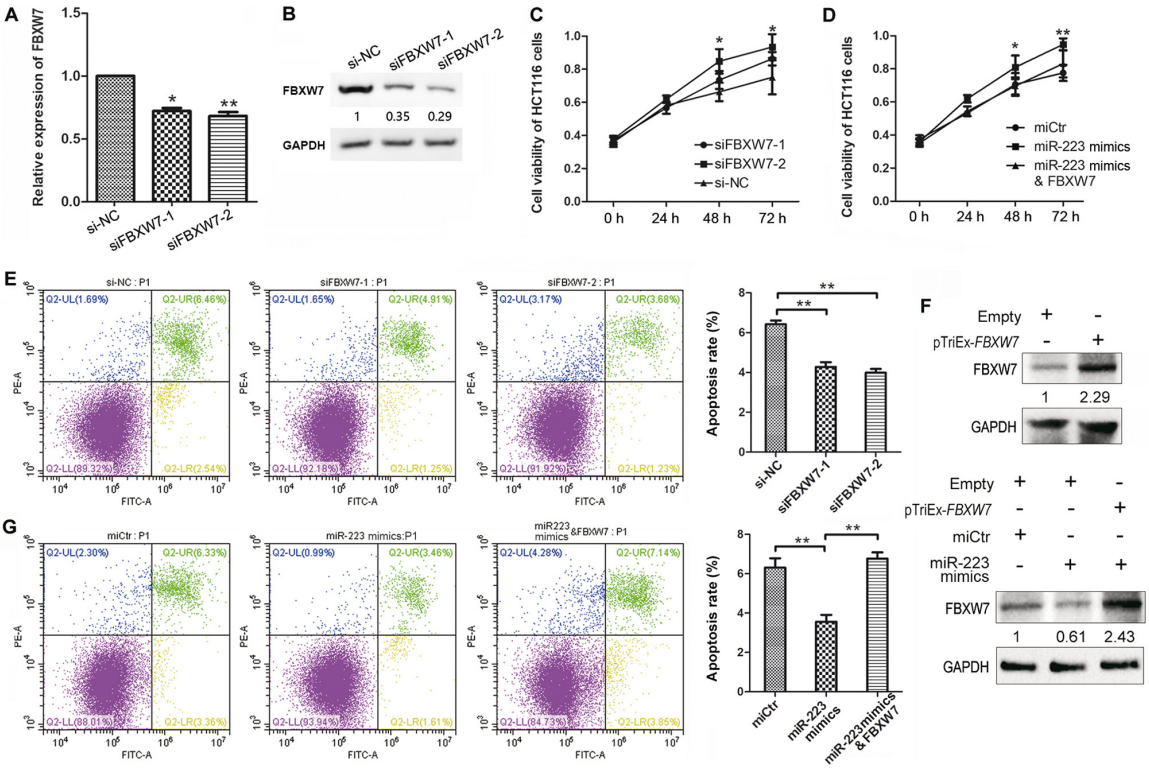

Figure 5. Effect of *FBXW7* knockdown on the viability and apoptosis of HCT116 cells. (A) FBXW7 mRNA expression levels in HCT116 cells transfected with siRNA targeting *FBXW7* or si-NC. (B) FBXW7 protein expression levels were detected by western blotting. (C) HCT116 cell viability following transfection with siFBXW7-1 and -2, or si-NC. (D) Cell viability following transfection with miR-223 mimics, miCtr or co-transfection with miR-223 mimics and FBXW7 overexpression plasmid. (E) HCT116 cell apoptosis following transfection with siFBXW7. Apoptotic rates are calculated as the frequency of Annexin V^+PI^+ cells relative to total cells. (F) FBXW7 protein expression levels in HCT116 cells transfected with miR-223 mimics and FBXW7 overexpression plasmid. The upper panel shows overexpression of FBXW7 induced by pTriEx-*FBXW7* alone, the lower panel shows expression of FBXW7 in cells transfected with pTriEx-*FBXW7* and miR-223 mimics. (G) Apoptosis of HCT116 cells following transfection with miR-223 mimics, miCtr or co-transfection with miR-223 mimics and FBXW7 overexpression plasmid. Data are presented as the mean ± SD of three replicates. *P<0.05, **P<0.01 (one-way ANOVA and Tukey's post hoc test). miR, microRNA; FBXW7, F-box and WD repeat domain containing 7; miCtr, mimics control; si, small interfering RNA; NC, negative control; FITC, fluorescein isothiocyanate; PI, propidium iodide; UL, upper left; UR, upper right; LL, lower left; LR, lower right.

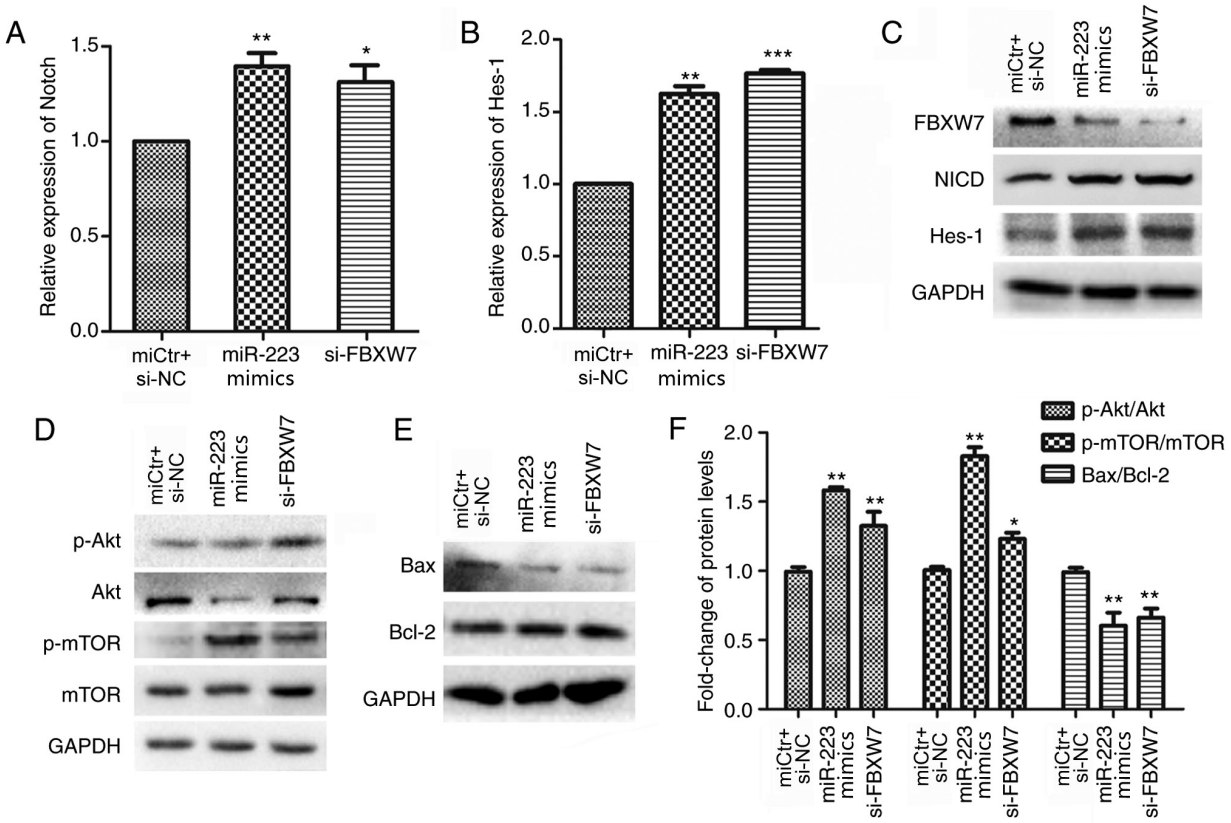

Figure 6. FBXW7 regulates the progression of CRC through the Notch and AKT/mTOR signalling pathways. Relative mRNA expression levels of *Notch* and *Hes-1* in HCT116 cells following (A) miR-223 mimics or (B) si*FBXW7*-2 transfection. miCtr + si-NC co-transfection was used as a control. (C) Protein expression levels of NICD and Hes-1 in HCT116 cells following miR-223 mimic or si*FBXW7*-2 transfection. (D) Protein expression levels of total Akt, p-Akt, mTOR and p-mTOR in HCT116 cells following miR-223 mimic or si*FBXW7*-2 transfection. (E) Protein expression levels of Bax and Bcl-2 after transfection with miR-223 mimics or si*FBXW7*-2 transfection. (F) Ratios of p-Akt/Akt, p-mTOR/mTOR and Bax/Bcl-2 calculated using the densitometric value of the protein bands, after normalization to GAPDH. Data are presented as the mean ± SD of three replicates. *P<0.05, **P<0.01, ***P<0.001, vs. control (one-way ANOVA and Tukey's post hoc test). miR, microRNA; FBXW7, F-box and WD repeat domain containing 7; si, small interfering RNA; Hes-1; hes family bHLH transcription factor 1; p, phosphorylated; NICD, Notch intracellular receptor domain.

mTOR and p-mTOR, as well as the upstream components of the mTOR pathway, Akt and p-Akt were also examined (Fig. 6D). Transfection with miR-223 mimics and si*FXBW7*-2 both increased the ratio of p-mTOR to total mTOR and the ratio of p-Akt to total Akt (Fig. 6F). In addition, the expression level of Bcl-2 was also upregulated following FBXW7 down-regulation either through miR-223 mimics or si*FXBW7*-2, while the levels of Bax were downregulated (Fig. 6E), and the ratio of Bax to Bcl-2 was decreased (Fig. 6F). These results demonstrated that *FBXW7* functioned through the Notch and Akt/mTOR signalling pathways.

Discussion

The tumour suppressor gene *FBXW7* has been reported to inhibit tumour progression by suppressing cell proliferation and inducing apoptosis (31,32). FBXW7 may be an independent factor affecting the survival of patients with CRC, and its expression has been reported to be associated with the occurrence, development and prognosis of CRC (33,34). Iwatsuki *et al* (35) detected the expression levels of FBXW7 mRNA and protein in 93 CRC samples and found that the expression of FBXW7 was lower in CRC tumour tissues than in adjacent tissue samples. Notably, patients with low expression of FBXW7 had a poor prognosis (35).

miR-223 is significantly associated with the tumour size and TNM stage of gastric cancer, as well as the invasion and distant metastasis of CRC (36,37). Therefore, miR-223 may have a role in the development of CRC, similar to miR-200a and miR-125b (38,39). *FBXW7* is one of the identified targets of various miRNAs (40,41). Sano *et al* (42) demonstrated that miR-25 could downregulate the expression of FBXW7, which may affect the proliferation, invasion and apoptosis of gastric cancer cells. In addition, a previous study confirmed that miR-25 and miR-223 could reduce the mRNA expression levels of *FBXW7*, which affects the activity of cyclin E and cell cycle progression (43). In the present study, inhibiting miR-223 increased the number of apoptotic cells, possibly as a result of endogenous FBXW7 reducing the activity of cyclin E through an as yet unknown mechanism that ultimately promotes cell apoptosis. Moreover, siRNA was used to directly interfere with the expression of FBXW7, resulting in increased HCT116 cell viability and inhibition of apoptosis. In addition, rescuing FBXW7 after miR-223 transfection produced the opposite result. This indicates that a direct relationship may exist between the proliferation and apoptosis of HCT116 cells and the effect of FBXW7.

miR-223 was upregulated in CRC tissues compared with normal tissues, whereas *FBXW7* was downregulated in CRC tissues. The important role of FBXW7 in human cancer

suggests that downregulation of FBXW7 through overexpression of miR-223 may become an important indicator of cancer development (44). Dysregulation of miR-223 can attenuate the tumour suppressor activity of FBXW7 during cell transformation (45). Therefore, further investigations of the function of FBXW7 and its downstream pathways in CRC progression are necessary. Blocking the Notch and mTOR pathways has been shown to affect the proliferation of various cancer cells, including endometrial carcinoma, breast cancer and retinoblastoma cells (46,47), indicating that these signalling pathways are involved in the development of these types of cancer. Previous studies have demonstrated that the Notch and NF-κB pathways are involved in cancer cell progression after transcriptionally regulating the expression of miR-223 (31,47). NICD, which is degraded by FBXW7, acts as a transcriptional activator that positively regulates target genes, including Hes-1. Hes-1 directly promotes cell proliferation (48). A recent study concluded that the active status of mTOR, p-mTOR, may be related to cell proliferation (23). In addition, Senoo *et al* (49) reported that Akt phosphorylation directly mediated Rho^{null} cell migration and apoptosis. Based on the aforementioned studies and the present results, it may be concluded that inhibition of FBXW7 expression by miR-223 promotes the proliferation and suppresses the apoptosis of HCT116 cells through the Notch and Akt/mTOR pathways. miR-223 has a positive impact on the Notch pathway and Akt/mTOR activation, and whether this effect is mediated directly by miR-223 or indirectly by FBXW7 after miR-223 binding needs to be further clarified.

In summary, the present study demonstrated that upregulated miR-223 binds to the 3'UTR of the *FBXW7* gene and inhibits the expression of FBXW7, ultimately promoting the proliferation and preventing the apoptosis of CRC cells through the Notch and Akt/mTOR signalling pathways. Further examination of the upstream molecular mechanism of miR-223 upregulation in CRC cells, and how FBXW7 affects cell invasion and migration, will lead to a better understanding of the occurrence and development of CRC and provide new insight for early screening and diagnosis of CRC.

Acknowledgements

Not applicable.

Funding

This study was funded by the Natural Science Foundation of Hubei Province (grant nos. 2018CFB185, 2018CFB093 and 2017CFB238), the Natural Science Foundation of Hubei Provincial Department of Education (grant nos. Q20192105 and Q20192104), the Faculty Development Grants of Hubei University of Medicine (grant nos. 2016QDJZR03 and 2017QDJZR08), and the Hubei Provincial Training Program of Innovation and Entrepreneurship for Undergraduates (grant nos. S201910929032 and S201913249006).

Availability of data and materials

The datasets used and/or analysed during the current study are available from the corresponding author on reasonable request.

Authors' contributions

LL and ZL contributed to the design of experiments. ZL, TM, JD and XL conducted the experiments. TM and XL provided reagents. JD and ZL analysed the data. LL and ZL wrote the paper. LL edited the paper. All authors read and approved the final manuscript.

Ethics approval and consent to participate

All procedures performed in the study involving human participants were approved by the ethics committee of Hubei University of Medicine, in accordance with the Declaration of Helsinki. Written informed consent was obtained from all participants.

Patient consent for publication

Not applicable.

Competing interests

The authors declare that they have no competing interests.

References

1. Chen W, Zheng R, Baade PD, Zhang S, Zeng H, Bray F, Jemal A, Yu XQ and He J: Cancer statistics in China, 2015. CA Cancer J Clin 66: 115-132, 2016.
2. Jemal A, Bray F, Center MM, Ferlay J, Ward E and Forman D: Global cancer statistics. CA Cancer J Clin 61: 69-90, 2011.
3. Zhang K, Song P, Gao J, Li G, Zhao X and Zhang S: Perspectives on a combined test of multi serum biomarkers in China: Towards screening for and diagnosing hepatocellular carcinoma at an earlier stage. Drug Discov Ther 8: 102-109, 2014.
4. Romano M, De Francesco F, Pirozzi G, Gringeri E, Boetto R, Di Domenico M, Zavan B, Ferraro GA and Cillo U: Expression of cancer stem cell biomarkers as a tool for a correct therapeutic approach to hepatocellular carcinoma. Oncoscience 2: 443-456, 2015.
5. Inuzuka H, Shaik S, Onoyama I, Gao D, Tseng A, Maser RS, Zhai B, Wan L, Gutierrez A, Lau AW, *et al*: SCF(FBW7) regulates cellular apoptosis by targeting MCL1 for ubiquitylation and destruction. Nature 471: 104-109, 2011.
6. Yeh CH, Bellon M and Nicot C: FBXW7: A critical tumor suppressor of human cancers. Mol Cancer 17: 115, 2018.
7. Takeishi S and Nakayama KI: Role of Fbxw7 in the maintenance of normal stem cells and cancer-initiating cells. Brit J Cancer 111: 1054-1059, 2014.
8. Davis RJ, Welcker M and Clurman BE: Tumor suppression by the Fbw7 ubiquitin ligase: Mechanisms and opportunities. Cancer Cell 26: 455-464, 2014.
9. Kawashita Y, Morine Y, Ikemoto T, Saito Y, Iwahashi S, Yamada S, Higashijima J, Imura S, Ogawa H, Yagi T and Shimada M: Loss of Fbxw7 expression is a predictor of recurrence in colorectal liver metastasis. J Hepatobiliary Pancreat Sci 24: 576-583, 2017.
10. Zhao Y, Wang M, Cui C, Zhang L, Liao F, Li H and Wu X: Significance of combined tests of serum golgi glycoprotein 73 and other biomarkers in diagnosis of small primary hepatocellular carcinoma. Cancer Biomark 15: 677-683, 2015.
11. Wang X, Zhang J, Zhou L, Sun W, Zheng ZG, Lu P, Gao Y, Yang XS, Zhang ZC, Tao KS and Dou KF: Fbxw7 regulates hepatocellular carcinoma migration and invasion via Notch1 signaling pathway. Int J Oncol 47: 231-243, 2015.
12. Li G, Luna C, Qiu J, Epstein DL and Gonzalez P: Alterations in microRNA expression in stress-induced cellular senescence. Mech Ageing Dev 130: 731-741, 2009.
13. Ramalinga M, Roy A, Srivastava A, Bhattarai A, Harish V, Suy S, Collins S and Kumar D: MicroRNA-212 negatively regulates starvation induced autophagy in prostate cancer cells by inhibiting SIRT1 and is a modulator of angiogenesis and cellular senescence. Oncotarget 6: 34446-34457, 2015.

14. Hermeking H: MicroRNAs in the p53 network: Micromanagement of tumour suppression. Nat Rev Cancer 12: 613-626, 2012.
15. Welch C, Chen Y and Stallings RL: MicroRNA-34a functions as a potential tumor suppressor by inducing apoptosis in neuroblastoma cells. Oncogene 26: 5017-5022, 2007.
16. Li R, Wu S, Chen X, Xu H, Teng P and Li W: miR-223/FBW7 axis regulates doxorubicin sensitivity through epithelial mesenchymal transition in non-small cell lung cancer. Am J Transl Res 8: 2512-2524, 2016.
17. Ibusuki M, Yamamoto Y, Shinriki S, Ando Y and Iwase H: Reduced expression of ubiquitin ligase FBXW7 mRNA is associated with poor prognosis in breast cancer patients. Cancer Sci 102: 439-445, 2011.
18. Yu J, Zhang W, Gao F, Liu YX, Chen ZY, Cheng LY, Xie SF and Zheng SS: FBW7 increases chemosensitivity in hepatocellular carcinoma cells through suppression of epithelial-mesenchymal transition. Hepatobiliary Pancreat Dis Int 13: 184-191, 2014.
19. Ding J, Zhao Z, Song J, Luo B and Huang L: miR-223 promotes the doxorubicin resistance of colorectal cancer cells via regulating epithelial-mesenchymal transition by targeting FBXW7. Acta Biochim Biophys Sin (Shanghai) 50: 597-604, 2018.
20. Lu G and Wang J: Dynamic changes in routine blood parameters of a severe COVID-19 case. Clin Chim Acta 508: 98-102, 2020.
21. Gharaibeh L, Elmadany N, Alwosaibai K and Alshaer W: Notch1 in cancer therapy: Possible clinical implications and challenges. Mol Pharmacol 98: 559-576, 2020.
22. Vacca A, Felli MP, Palermo R, Di Mario G, Calce A, Di Giovine M, Frati L, Gulino A and Screpanti I: Notch3 and pre-TCR interaction unveils distinct NF-kappaB pathways in T-cell development and leukemia. EMBO J 25: 1000-1008, 2006.
23. Wu J, Lu AD, Zhang LP, Zuo YX and Jia YP: Study of clinical outcome and prognosis in pediatric core binding factor-acute myeloid leukemia. Zhonghua Xue Ye Xue Za Zhi 40: 52-57, 2019 (In Chinese).
24. Li Y, Guessous F, Zhang Y, Dipierro C, Kefas B, Johnson E, Marcinkiewicz L, Jiang J, Yang Y, Schmittgen TD, *et al*: MicroRNA-34a inhibits glioblastoma growth by targeting multiple oncogenes. Cancer Res 69: 7569-7576, 2009.
25. Ji Q, Hao X, Zhang M, Tang W, Yang M, Li L, Xiang D, Desano JT, Bommer GT, Fan D, *et al*: MicroRNA miR-34 inhibits human pancreatic cancer tumor-initiating cells. PLoS One 4: e6816, 2009.
26. Xiao G, Li Y, Wang M, Li X, Qin S, Sun X, Liang R, Zhang B, Du N, Xu C, *et al*: FBXW7 suppresses epithelial-mesenchymal transition and chemo-resistance of non-small-cell lung cancer cells by targeting snail for ubiquitin-dependent degradation. Cell Prolif 51: e12473, 2018.
27. Livak KJ and Schmittgen TD: Analysis of relative gene expression data using real-time quantitative PCR and the 2(-Delta Delta C(T)) method. Methods 25: 402-408, 2001.
28. Agarwal V, Bell GW, Nam J and Bartel DP: Predicting effective microRNA target sites in mammalian mRNAs. eLife, 4: e05005, 2015.
29. Bilinska K, Jakubowska P, Von Bartheld CS and Butowt R: Expression of the SARS-CoV-2 entry proteins, ACE2 and TMPRSS2, in cells of the olfactory epithelium: Identification of cell types and trends with age. ACS Chem Neurosci 11: 1555-1562, 2020.
30. Thompson WW, Shay DK, Weintraub E, Brammer L, Cox N, Anderson LJ and Fukuda K: Mortality associated with influenza and respiratory syncytial virus in the United States. JAMA 289: 179-186, 2003.
31. Zhang H, Chen F, He Y, Yi L, Ge C, Shi X, Tang C, Wang D, Wu Y and Nian W: Sensitivity of non-small cell lung cancer to erlotinib is regulated by the Notch/miR-223/FBXW7 pathway. Biosci Rep 37: BSR20160478, 2017.
32. Sun XF, Sun JP, Hou HT, Li K, Liu X and Ge QX: MicroRNA-27b exerts an oncogenic function by targeting Fbxw7 in human hepatocellular carcinoma. Tumour Biol 37: 15325-15332, 2016.
33. Kurashige J, Watanabe M, Iwatsuki M, Kinoshita K, Saito S, Hiyoshi Y, Kamohara H, Baba Y, Mimori K and Baba H: Overexpression of microRNA-223 regulates the ubiquitin ligase FBXW7 in oesophageal squamous cell carcinoma. Br J Cancer 106: 182-188, 2012.
34. Wang Y, Liu Y, Lu J, Zhang P, Wang Y, Xu Y, Wang Z, Mao JH and Wei G: Rapamycin inhibits FBXW7 loss-induced epithelial-mesenchymal transition and cancer stem cell-like characteristics in colorectal cancer cells. Biochem Biophys Res Commun 434: 352-356, 2013.
35. Iwatsuki M, Mimori K, Ishii H, Yokobori T, Takatsuno Y, Sato T, Toh H, Onoyama I, Nakayama KI, Baba H and Mori M: Loss of FBXW7, a cell cycle regulating gene, in colorectal cancer: Clinical significance. Int J Cancer 126: 1828-1837, 2010.
36. Huang Z, Huang D, Ni S, Peng Z, Sheng W and Du X: Plasma microRNAs are promising novel biomarkers for early detection of colorectal cancer. Int J Cancer 127: 118-126, 2010.
37. Li ZW, Yang YM, Du LT, Dong Z, Wang LL, Zhang X, Zhou XJ, Zheng GX, Qu AL and Wang CX: Overexpression of miR-223 correlates with tumor metastasis and poor prognosis in patients with colorectal cancer. Med Oncol 31: 256, 2014.
38. Pichler M, Ress AL, Winter E, Stiegelbauer V, Karbiener M, Schwarzenbacher D, Scheideler M, Ivan C, Jahn SW, Kiesslich T, *et al*: miR-200a regulates epithelial to mesenchymal transition-related gene expression and determines prognosis in colorectal cancer patients. Br J Cancer 110: 1614-1621, 2014.
39. Nishida N, Yokobori T, Mimori K, Sudo T, Tanaka F, Shibata K, Ishii H, Doki Y, Kuwano H and Mori M: MicroRNA miR-125b is a prognostic marker in human colorectal cancer. Int J Oncol 38: 1437-1443, 2011.
40. He D, Huang C, Zhou Q, Liu D, Xiong L, Xiang H, Ma G and Zhang Z: HnRNPK/miR-223/FBXW7 feedback cascade promotes pancreatic cancer cell growth and invasion. Oncotarget 8: 20165-20178, 2017.
41. Liu Z, Liu X, Liu S and Cao Q: Cholesterol promotes the migration and invasion of renal carcinoma cells by regulating the KLF5/miR-27a/FBXW7 pathway. Biochem Biophys Res Commun 502: 69-75, 2018.
42. Sano H, Kawahito Y, Wilder RL, Hashiramoto A, Mukai S, Asai K, Kimura S, Kato H, Kondo M and Hla T: Expression of cyclooxygenase-1 and -2 in human colorectal cancer. Cancer Res 55: 3785-3789, 1995.
43. Xu Y, Sengupta T, Kukreja L and Minella AC: MicroRNA-223 regulates cyclin E activity by modulating expression of F-box and WD-40 domain protein 7. J Biol Chem 285: 34439-34446, 2010.
44. Yeh CH, Bellon M, Pancewicz-Wojtkiewicz J and Nicot C: Oncogenic mutations in the FBXW7 gene of adult T-cell leukemia patients. Proc Natl Acad Sci USA 113: 6731-6736, 2016.
45. Hua J, Ding T and Yang L: Dysfunction of microRNA-32 regulates ubiquitin ligase FBXW7 in multiple myeloma disease. Onco Targets Ther 9: 6573-6579, 2016.
46. Thomas MR, Marston L, Rafferty GF, Calvert S, Marlow N, Peacock JL and Greenough A: Respiratory function of very prematurely born infants at follow up: Influence of sex. Arch Dis Child Fetal Neonatal Ed 91: F197-F201, 2006.
47. Kumar V, Palermo R, Talora C, Campese AF, Checquolo S, Bellavia D, Tottone L, Testa G, Miele E, Indraccolo S, *et al*: Notch and NF-kB signaling pathways regulate miR-223/FBXW7 axis in T-cell acute lymphoblastic leukemia. Leukemia 28: 2324-2335, 2014.
48. Espinosa L, Cathelin S, D'Altri T, Trimarchi T, Statnikov A, Guiu J, Rodilla V, Inglés-Esteve J, Nomdedeu J, Bellosillo B, *et al*: The Notch/Hes1 pathway sustains NF-κB activation through CYLD repression in T cell leukemia. Cancer Cell 18: 268-281, 2010.
49. Senoo H, Kamimura Y, Kimura R, Nakajima A, Sawai S, Sesaki H and Iijima M: Phosphorylated Rho-GDP directly activates mTORC2 kinase towards AKT through dimerization with Ras-GTP to regulate cell migration. Nat Cell Biol 21: 867-878, 2019.